

Search for a Higgs Boson Decaying into Two Photons at LEP

The L3 Collaboration

Abstract

A Higgs particle produced in association with a Z boson and decaying into two photons is searched for in the data collected by the L3 experiment at LEP. All possible decay modes of the Z boson are investigated. No signal is observed in 447.5 pb^{-1} of data recorded at centre-of-mass energies from 192 GeV up to 209 GeV. Limits on the branching fraction of the Higgs boson decay into two photons as a function of the Higgs mass are derived. A lower limit on the mass of a fermiophobic Higgs boson is set at 105.4 GeV at 95% confidence level.

Submitted to *Phys. Lett. B*

Introduction

The Standard Model of the electroweak interactions allows the decay of a Higgs boson h into a photon pair only at the one loop level. The branching fraction of this decay is small [1]. It amounts to about 0.1% for Higgs masses m_h between 80 and 110 GeV. Several extensions of the Standard Model predict enhancements of this branching fraction [2]. For instance, an appropriate choice of the parameters of the Two Higgs Doublet Models of Type I [3], predicts the lightest CP even Higgs not to couple to fermions at tree level. Such a Higgs is expected to decay dominantly into a pair of photons if its mass is below 90 GeV [4]. In Higgs triplet models, one of the neutral scalars may have a large branching fraction $BR(h \rightarrow \gamma\gamma)$ and be produced at LEP with rates comparable to the Standard Model ones [5]. At higher masses, the branching fraction $BR(h \rightarrow \gamma\gamma)$ decreases to the advantage of the $W^\pm W^{\mp*}$ mode.

This letter presents the search for a Higgs boson produced in association with a Z boson through the process $e^+e^- \rightarrow Zh$, followed by the decay $h \rightarrow \gamma\gamma$. All decay modes of the Z boson are investigated.

The high energy data sample collected by the L3 detector [6] at centre-of-mass \sqrt{s} up to 209 GeV is analysed. Results from partial samples were previously reported by L3 [7, 8] and other LEP Collaborations [9].

Data and Monte Carlo Samples

We analyse data collected with the L3 detector during the years 1999 and 2000 at centre-of-mass energies $\sqrt{s} = 192 - 209$ GeV, for a total integrated luminosity of 447.5 pb^{-1} . The data are grouped into ten samples whose average centre-of-mass energies and corresponding integrated luminosities are listed in Table 1. Results from 176 pb^{-1} of integrated luminosity collected at $\sqrt{s} = 189$ GeV are included in the final results.

The Standard Model Higgs production cross section is calculated using the HZHA generator [10]. Signal Monte Carlo samples are generated using PYTHIA [11] for Higgs masses between 50 and 120 GeV. These samples comprise between 500 and 2000 signal events depending on the search channel. For background studies the following Monte Carlo programs are used: KK2f [12] ($e^+e^- \rightarrow q\bar{q}(\gamma)$, $e^+e^- \rightarrow \mu^+\mu^-(\gamma)$, $e^+e^- \rightarrow \tau^+\tau^-(\gamma)$), PYTHIA ($e^+e^- \rightarrow ZZ$ and $e^+e^- \rightarrow Ze^+e^-$), KORALW [13] ($e^+e^- \rightarrow W^+W^-$), PHOJET [14] ($e^+e^- \rightarrow e^+e^-q\bar{q}$), KORALZ [15] ($e^+e^- \rightarrow \nu\bar{\nu}(\gamma)$), GGG [16] ($e^+e^- \rightarrow \gamma\gamma(\gamma)$), BHWIDE [17] ($e^+e^- \rightarrow e^+e^-(\gamma)$), TEEGG [18] ($e^+e^- \rightarrow e^+e^-\gamma$), DIAG36 [19] ($e^+e^- \rightarrow e^+e^-e^+e^-$) and EXCALIBUR [20] for other four-fermion final states. The number of simulated events for the most important background channels is at least 100 times higher than the corresponding number of expected events in the data.

The L3 detector response is simulated using the GEANT [21] program, which takes into account the effects of energy loss, multiple scattering and showering in the detector. The GHEISHA [22] package is used to simulate hadronic interactions in the detector. Time dependent inefficiencies, as monitored during the data acquisition period, are also simulated.

Analysis Procedure

The analysis aims to select events with isolated photons and a Z boson. Three final states are then investigated, according to the Z boson decay. They are denoted as $q\bar{q}\gamma\gamma$, $\nu\bar{\nu}\gamma\gamma$ and

$\ell^+\ell^-\gamma\gamma$, with $\ell = e, \mu, \tau$. The selections for each final state are described in the following and proceed from a common photon identification.

Photons are selected from clusters in the BGO electromagnetic calorimeter with an energy greater than 1 GeV and a shower profile compatible with that expected for an electromagnetic particle. The ratio of the energies measured in a 3×3 and a 5×5 matrix, centred on the most energetic crystal, must exceed 0.95. The energy deposit in the hadron calorimeter is required to be below 20% of the energy measured in the electromagnetic calorimeter.

No track should point to the clusters within 50 mrad in the plane perpendicular to the beam axis. Only clusters in the polar angle ranges $25^\circ < \theta < 35^\circ$, $45^\circ < \theta < 135^\circ$ and $145^\circ < \theta < 155^\circ$ are considered, well within the coverage of the barrel and end-cap regions of the BGO electromagnetic calorimeter. The distribution of the polar angle of the most energetic photon is shown in Figure 1.

These analyses require at least two photons. Photons from the decay of a heavy resonance are expected to be relatively energetic, hence the energy of the hardest photon has to exceed 10 GeV and the energy of the second most energetic photon has to exceed 6 GeV.

The $q\bar{q}\gamma\gamma$ Final State

Candidates in the $q\bar{q}\gamma\gamma$ final state are characterised by a pair of isolated photons accompanied by two jets. The $q\bar{q}\gamma\gamma$ selection starts from a preselection of hadronic events: high multiplicity events are required to be balanced and their visible energy E_{vis}/\sqrt{s} has to be larger than 0.5. The background from two-photon interaction events is reduced requiring the energy in a 30° cone around the beam pipe to be less than half of the visible energy. The preselection yield is reported in Table 2. Figure 2 shows the comparison between data and the Monte Carlo expectations for the distribution of E_{vis}/\sqrt{s} for the preselected events.

Events which contain at least two photons are selected. In addition, photons coming from neutral hadron decays are rejected by requiring the energy in a 10° cone around the photon direction to be less than 2.5 GeV, and that in a 20° cone to be less than 4.5 GeV. The number of charged tracks and calorimeter clusters in a 20° cone around the photon direction must be below four. The opening angle between the photons must be larger than 50° . All other particles are clustered into two jets using the DURHAM jet algorithm [23] and no jet is allowed within 25° around any photon.

The energy spectrum of the most energetic photon, normalised to the beam energy, before the application of any selection requirement on the photon energies, is shown in Figure 3a. Figure 3b presents the distribution of the recoil mass against the di-photon system after the cuts on the photon energies.

Finally, the recoil mass against the di-photon system is required to be consistent with the Z mass within 15 GeV. The efficiency is 40% for a Higgs boson mass of 100 GeV produced at $\sqrt{s} = 192$ GeV, and 47% for a Higgs of 110 GeV produced at $\sqrt{s} = 208$ GeV. The selection yield is presented in Table 2. 28 events are observed in the data, with 31 expected from Monte Carlo, mainly from the $e^+e^- \rightarrow q\bar{q}(\gamma)$ process.

The event with the highest value of the di-photon invariant mass is displayed in Figure 4. It was collected at $\sqrt{s} = 205.1$ GeV and its di-photon invariant mass is 111.8 ± 1.0 GeV while the recoil mass against the di-photon system is 87.1 ± 0.8 GeV.

The $\nu\bar{\nu}\gamma\gamma$ Final State

The signature of the $\nu\bar{\nu}\gamma\gamma$ final state consists in two photons and missing energy. Events are selected that have an identified photon pair, no charged tracks and an additional energy below 10 GeV. To ensure that the missing momentum is well contained in the detector, the absolute value of the cosine of its polar angle must not exceed 0.96. To reduce contributions from the $e^+e^- \rightarrow \gamma\gamma(\gamma)$ process and from double radiative events with final state particles escaping detection, the photon acoplanarity is required to exceed 3° . The distribution of this acoplanarity for the data and the Monte Carlo predictions is presented in Figure 5a. The total transverse momentum of the di-photon system must be greater than 2 GeV.

Figure 5b shows the distribution of the recoil mass against the two most energetic photons after selection requirements on all the other variables. As final selection criterium, this mass has to be consistent with the Z boson mass within 15 GeV. The efficiency is 47% for a Higgs boson mass of 100 GeV produced at $\sqrt{s} = 192$ GeV and 51% for a Higgs of 110 GeV produced at $\sqrt{s} = 206$ GeV. The number of selected events in data is 9 and 9.2 events are expected from the $e^+e^- \rightarrow \nu\bar{\nu}(\gamma)$ process. Other backgrounds are negligible.

The $\ell^+\ell^-\gamma\gamma$ Final State

The $\ell^+\ell^-\gamma\gamma$ final state has the characteristic signature of a photon pair and a lepton pair. Its selection proceeds from low multiplicity events with two identified photons and an associated lepton pair, selected as follows.

Electrons are identified from clusters in the electromagnetic calorimeter with an energy greater than 3 GeV and associated to a charged track. The energy deposit in the hadron calorimeter must be consistent with the tail of an electromagnetic shower. Less than 3 GeV are allowed in the electromagnetic calorimeter in a 10° cone around the electron direction. To increase efficiency, events with just one identified electron are also accepted.

Muons are identified from tracks in the muon chambers with a distance to the interaction vertex in the $r - \phi$ plane below 300 mm and a momentum above 3 GeV. The calorimetric energy in a 10° cone around the muon direction must not exceed 3 GeV. Events with one muon and one minimum ionising particle in the calorimeters are also accepted, as well as events with a single muon. The background from cosmic rays is rejected by requiring at least one hit in the scintillation counters in a 5 ns window around the beam crossing time.

Taus are identified as jets with one or three tracks in a 10° cone with an energy above 3 GeV. The energy in the $10^\circ - 30^\circ$ cone around the tau direction has to be below 30% of the energy in the $0^\circ - 10^\circ$ cone. Events with only one identified tau lepton are also accepted.

The preselection of $\ell^+\ell^-\gamma\gamma$ events yields the results listed in Table 3. Double radiative di-lepton events are the dominant background and are rejected further by requiring the energy of the most energetic lepton to be below 80 GeV.

The distribution of the energy of the second most energetic photon normalised to the beam energy is presented in Figure 6a for the preselected events. Figure 6b shows the recoil mass against the photons after all selection criteria but the recoil mass.

The final selection requirement imposes the recoil mass to be consistent with the Z mass within 15 GeV. At centre-of-mass energies below $\sqrt{s} = 202$ GeV the presence of two identified leptons is enforced. Their invariant mass is required to be between 81 and 101 GeV and the selection criterium on the recoil mass is relaxed.

The efficiency varies from 31% for a Higgs boson mass of 100 GeV produced at $\sqrt{s} = 192$ GeV, to 43% for a Higgs of 110 GeV produced at $\sqrt{s} = 208$ GeV. The yield of this

selection is presented in Table 3. 7 events are observed in the data, with 8.0 expected from Monte Carlo, mainly from the $e^+e^- \rightarrow \ell^+\ell^-(\gamma)$ processes.

Results

No significant excess indicating the production of a Higgs boson decaying into two photons is observed in the data. The confidence level [24] for the absence of a Higgs signal is then calculated from the reconstructed di-photon invariant mass as the final discriminant variable. This distribution is shown in Figure 7a for the data analysed in this paper, collected at $\sqrt{s} = 192 - 209$ GeV and in Figure 7b including the data collected at $\sqrt{s} = 189$ GeV.

The calculation of the limits takes into account systematic uncertainties of 2% on the signal expectations and 8% on the background. The signal uncertainty follows from the Monte Carlo statistics that also accounts for a 4% uncertainty on the background. Another uncertainty of 7% is assigned to the background normalisation for hadronic events with photons. A variation of 2% of the calorimetric energy scale has little effect on the limits. The effects of the energy and angular resolutions of the photons and the systematic uncertainty on the integrated luminosity are also found to be negligible.

Figure 8 presents the upper limit on the branching fraction $BR(h \rightarrow \gamma\gamma)$ as a function of the Higgs mass, assuming the Standard Model cross section for the Zh production. The expected limit is also shown together with the theoretical prediction for a fermiophobic Higgs boson as calculated with the HDECAY program [25]. Previous L3 results [8] are included in the calculation of this limit. The observed limit for $BR(h \rightarrow \gamma\gamma) = 1$ is 114 GeV.

The lower limit on the mass of a fermiophobic Higgs boson is set at

$$m_h > 105.4 \text{ GeV at 95\% confidence level,}$$

to be compared with the expected mass limit of 105.3 GeV.

References

- [1] J. Ellis, M.K. Gaillard and P.V. Nanopoulos, Nucl. Phys. **B 106** (1976) 292.
- [2] K. Hagiwara, R. Szalapski, D. Zeppenfeld, Phys. Lett. **B 318** (1993) 155; K. Hagiwara and M.L. Stong, Z. Phys. **C 62** (1994) 99; A.G. Akeroyd, Phys. Lett. **B 368** (1996) 89; A. Stange, W. Marciano and S. Willenbrock, Phys. Rev. **D 49** (1994) 1354; H. Haber, G. Kane and T. Sterling, Nucl. Phys. **B 161** (1979) 493; J.F. Gunion, R. Vega and J. Wudka, Phys. Rev. **D 42** (1990) 1673.
- [3] L. Brücher and R. Santos, Eur. Phys. J. **C 12** (2000) 87.
- [4] M.A. Diaz and T.J. Weiler, preprint hep-ph/9401259 (1994).
- [5] P. Bamert and Z. Kunszt, Phys. Lett. **B 306** (1993) 335.
- [6] L3 Collab., B. Adeva *et al.*, Nucl. Instr. and Meth. **A 289** (1990) 35; M. Chemarin *et al.*, Nucl. Instr. and Meth. **A 349** (1994) 345; M. Acciarri *et al.*, Nucl. Instr. and Meth. **A 351** (1994) 300; G. Basti *et al.*, Nucl. Instr. and Meth. **A 374** (1996) 293; I.C. Brock *et al.*, Nucl. Instr. and Meth. **A 381** (1996) 236; A. Adam *et al.*, Nucl. Instr. and Meth. **A 383** (1996) 342.
- [7] L3 Collab., O. Adriani *et al.*, Phys. Lett. **B 292** (1992) 472; L3 Collab., M. Acciarri *et al.*, Phys. Lett. **B 388** (1996) 409.
- [8] L3 Collab., M. Acciarri *et al.*, Phys. Lett. **B 489** (2000) 115.
- [9] ALEPH Collab., R. Barate *et al.*, Phys. Lett. **B 487** (2000) 241. DELPHI Collab., P. Abreu *et al.*, Phys. Lett. **B 458** (1999) 431. DELPHI Collab., P. Abreu *et al.*, Phys. Lett. **B 507** (2001) 89. OPAL Collab., K. Ackerstaff *et al.*, Phys. Lett. **B 437** (1998) 218; OPAL Collab., G. Abbiendi *et al.*, Phys. Lett. **B 464** (1999) 311.
- [10] P. Janot, “The HZHA generator”, in “Physics at LEP2”, Eds. G. Altarelli, T. Sjöstrand and F. Zwirner, Report CERN 96-01 (1996) Vol.2, 309.
- [11] T. Sjöstrand, Preprint CERN-TH/7112/93 (1993), revised August 1995; T. Sjöstrand, Comp. Phys. Comm. **82** (1994) 74.
- [12] S. Jadach, B.F.L. Ward and Z. Wąs, Comp. Phys. Comm. **130** (2000) 260.
- [13] M. Skrzypek *et al.*, Comp. Phys. Comm. **94** (1996) 216; M. Skrzypek *et al.*, Phys. Lett. **B 372** (1996) 289.
- [14] R. Engel, Z. Phys. **C 66** (1995) 203; R. Engel, J. Ranft and S. Roesler, Phys. Rev. **D 52** (1995) 1459.
- [15] S. Jadach, B.F.L. Ward and Z. Wąs, Comp. Phys. Comm. **79** (1994) 503.
- [16] F.A. Berends and R. Kleiss, Nucl. Phys. **B 186** (1981) 22.
- [17] S. Jadach *et al.*, Phys. Lett. **B 390** (1997) 298.
- [18] D. Karlen, Nucl. Phys. **B 289** (1987) 23.

- [19] F.A. Berends, P.H. Daverveldt and R. Kleiss, Nucl. Phys. **B** **253** (1985) 441.
- [20] F.A. Berends, R. Pittau and R. Kleiss, Comp. Phys. Comm. **85** (1995) 437.
- [21] R. Brun *et al.*, Preprint CERN DD/EE/84-1 (1984), revised 1987.
- [22] H. Fesefeldt, RWTH Aachen Report PITHA 85/02 (1985).
- [23] S. Bethke *et al.*, Nucl. Phys. **B** **370** (1992) 310 and references therein.
- [24] The LEP Working Group for Higgs Boson Searches and the ALEPH, DELPHI, L3 and OPAL Collaborations, preprint CERN-EP/2000-55 (2000).
- [25] A. Djouadi, J. Kalinowski and M. Spira, Comp. Phys. Comm. **108** (1998) 56.

The L3 Collaboration:

P.Achard,²⁰ O.Adriam,¹⁷ M.Aguilar-Benitez,²⁴ J.Alcaraz,^{24,18} G.Alemanni,²² J.Allaby,¹⁸ A.Aloisio,²⁸ M.G.Alvaggi,²⁸ H.Anderhub,⁴⁶ V.P.Andreev,^{6,33} F.Anselmo,⁹ A.Arefiev,²⁷ T.Azemoon,³ T.Aziz,^{10,18} P.Bagnaia,³⁸ A.Bajo,²⁴ G.Baksay,¹⁶ L.Baksay,²⁵ S.V.Baldew,² S.Banerjee,¹⁰ Sw.Banerjee,⁴ A.Barczyk,^{46,44} R.Barillère,¹⁸ P.Bartalini,²² M.Basile,⁹ N.Batalova,⁴³ R.Battiston,³² A.Bay,²² F.Becattini,¹⁷ U.Becker,¹⁴ F.Behner,⁴⁶ L.Bellucci,¹⁷ R.Berbeco,³ J.Berdugo,²⁴ P.Berges,¹⁴ B.Bertucci,³² B.L.Betev,⁴⁶ M.Biasini,³² M.Biglietti,²⁸ A.Biland,⁴⁶ J.J.Blaising,⁴ S.C.Blyth,³⁴ G.J.Bobbink,² A.Böhm,¹ L.Boldizsar,¹³ B.Borgia,³⁸ S.Bottai,¹⁷ D.Bourilkov,⁴⁶ M.Bourquin,²⁰ S.Braccini,²⁰ J.G.Branson,⁴⁰ F.Brochu,⁴ J.D.Burger,¹⁴ W.J.Burger,³² X.D.Cai,¹⁴ M.Capell,¹⁴ G.Cara Romeo,⁹ G.Carlino,²⁸ A.Cartacci,¹⁷ J.Casaus,²⁴ F.Cavallari,³⁸ N.Cavallo,³⁵ C.Cecchi,³² M.Cerrada,²⁴ M.Chamizo,²⁰ Y.H.Chang,⁴⁸ M.Chemarin,²³ A.Chen,⁴⁸ G.Chen,⁷ G.M.Chen,⁷ H.F.Chen,²¹ H.S.Chen,⁷ G.Chiefari,²⁸ L.Cifarelli,³⁹ F.Cindolo,⁹ I.Clare,¹⁴ R.Clare,³⁷ G.Coignet,⁴ N.Colino,²⁴ S.Costantini,³⁸ B.de la Cruz,²⁴ S.Cucciarelli,³² J.A.van Dalen,³⁰ R.de Asmundis,²⁸ P.Déglon,²⁰ J.Debreczeni,¹³ A.Degré,⁴ K.Deiters,⁴⁴ D.della Volpe,²⁸ E.Delmeire,²⁰ P.Denes,³⁶ F.DeNotaristefani,³⁸ A.De Salvo,⁴⁶ M.Diemoz,³⁸ M.Dierckxsens,² C.Dionisi,³⁸ M.Dittmar,^{46,18} A.Doria,²⁸ M.T.Dova,^{11,‡} D.Duchesneau,⁴ B.Echenard,²⁰ A.Eline,¹⁸ H.El Mamouni,²³ A.Engler,³⁴ F.J.Eppling,¹⁴ A.Ewers,¹ P.Extermann,²⁰ M.A.Falagan,²⁴ S.Falciano,³⁸ A.Favara,³¹ J.Fay,²³ O.Fedin,³³ M.Felcini,⁴⁶ T.Ferguson,³⁴ H.Fesefeldt,¹ E.Fiandrini,³² J.H.Field,²⁰ F.Filthaut,³⁰ P.H.Fisher,¹⁴ W.Fisher,³⁶ I.Fisk,⁴⁰ G.Forconi,¹⁴ K.Freudenreich,⁴⁶ C.Furetta,²⁶ Yu.Galaktionov,^{27,14} S.N.Ganguli,¹⁰ P.Garcia-Abia,^{5,18} M.Gataullin,³¹ S.Gentile,³⁸ S.Giagu,³⁸ Z.F.Gong,²¹ G.Grenier,²³ O.Grimm,⁴⁶ M.W.Gruenewald,¹ M.Guida,³⁹ R.van Gulik,² V.K.Gupta,³⁶ A.Gurtu,¹⁰ L.J.Gutay,⁴³ D.Haas,⁵ R.Sh.Hakobyan,³⁰ D.Hatzifotiadou,⁹ T.Hebbeker,¹ A.Hervé,¹⁸ J.Hirschfelder,³⁴ H.Hofer,⁴⁶ M.Hohlmann,²⁵ G.Holzner,⁴⁶ S.R.Hou,⁴⁸ Y.Hu,³⁰ B.N.Jin,⁷ L.W.Jones,³ P.de Jong,² I.Josa-Mutuberriá,²⁴ D.Käfer,¹ M.Kaur,¹⁵ M.N.Kienzle-Focacci,²⁰ J.K.Kim,⁴² J.Kirkby,¹⁸ W.Kittel,³⁰ A.Klimentov,^{14,27} A.C.König,³⁰ M.Kopal,⁴³ V.Koutsenko,^{14,27} M.Kräber,⁴⁶ R.W.Kraemer,³⁴ W.Krenz,¹ A.Krüger,⁴⁵ A.Kunin,¹⁴ P.Ladron de Guevara,²⁴ I.Laktineh,²³ G.Landi,¹⁷ M.Lebeau,¹⁸ A.Lebedev,¹⁴ P.Lebrun,²³ P.Lecomte,⁴⁶ P.Lecoq,¹⁸ P.Le Coultre,⁴⁶ J.M.Le Goff,¹⁸ R.Leiste,⁴⁵ M.Levtchenko,²⁶ P.Levtchenko,³³ C.Li,²¹ S.Likhoded,⁴⁵ C.H.Lin,⁴⁸ W.T.Lin,⁴⁸ F.L.Linde,² L.Lista,²⁸ Z.A.Liu,⁷ W.Lohmann,⁴⁵ E.Longo,³⁸ Y.S.Lu,⁷ K.Lübelsmeyer,¹ C.Luci,³⁸ L.Luminari,³⁸ W.Lustermann,⁴⁶ W.G.Ma,²¹ L.Malgeri,²⁰ A.Malinin,²⁷ C.Maňa,²⁴ D.Mangeol,³⁰ J.Mans,³⁶ J.P.Martin,²³ F.Marzano,³⁸ K.Mazumdar,¹⁰ R.R.McNeil,⁶ S.Mele,^{18,28} L.Merola,²⁸ M.Meschini,¹⁷ W.J.Metzger,³⁰ A.Mihul,¹² H.Milcent,¹⁸ G.Mirabelli,³⁸ J.Mnich,¹ G.B.Mohanty,¹⁰ G.S.Muanza,²³ A.J.M.Muijs,² B.Musicar,⁴⁰ M.Musy,³⁸ S.Nagy,¹⁶ S.Natale,²⁰ M.Napolitano,²⁸ F.Nessi-Tedaldi,⁴⁶ H.Newman,³¹ T.Niessen,¹ A.Nisati,³⁸ H.Nowak,⁴⁵ R.Ofierzynski,⁴⁶ G.Organtini,³⁸ C.Palomares,¹⁸ D.Pandoulas,¹ P.Paolucci,²⁸ R.Paramatti,³⁸ G.Passaleva,¹⁷ S.Patricelli,²⁸ T.Paul,¹¹ M.Pauluzzi,³² C.Paus,¹⁴ F.Pauss,⁴⁶ M.Pedace,³⁸ S.Pensotti,²⁶ D.Perret-Gallix,⁴ B.Petersen,³⁰ D.Piccolo,²⁸ F.Pierella,⁹ M.Pioppi,³² P.A.Piroué,³⁶ E.Pistolesi,²⁶ V.Plyaskin,²⁷ M.Pohl,²⁰ V.Pojidaev,¹⁷ J.Pothier,¹⁸ D.O.Prokofiev,⁴³ D.Prokofiev,³³ J.Quartieri,³⁹ G.Rahal-Callot,⁴⁶ M.A.Rahaman,¹⁰ P.Raics,¹⁶ N.Raja,¹⁰ R.Ramelli,⁴⁶ P.G.Rancoita,²⁶ R.Ranieri,¹⁷ A.Raspereza,⁴⁵ P.Razis,²⁹ D.Ren,⁴⁶ M.Rescigno,³⁸ S.Reucroft,¹¹ S.Riemann,⁴⁵ K.Riles,³ B.P.Roe,³ L.Romero,²⁴ A.Rosca,⁸ S.Rosier-Lees,⁴ S.Roth,¹ C.Rosenbleck,¹ B.Roux,³⁰ J.A.Rubio,¹⁸ G.Ruggiero,¹⁷ H.Rykaczewski,⁴⁶ A.Sakharov,⁴⁶ S.Saremi,⁶ S.Sarkar,³⁸ J.Salicio,¹⁸ E.Sánchez,²⁴ M.P.Sanders,³⁰ C.Schäfer,¹⁸ V.Schegelsky,³³ S.Schmidt-Kærst,¹ D.Schmitz,¹ H.Schopper,⁴⁷ D.J.Schotanus,³⁰ G.Schowering,¹ C.Sciacca,²⁸ L.Servoli,³² S.Shevchenko,³¹ N.Shivarov,⁴¹ V.Shoutko,¹⁴ E.Shumilov,²⁷ A.Shvorob,³¹ T.Siedenburg,¹ D.Son,⁴² P.Spillantini,¹⁷ M.Steuer,¹⁴ D.P.Stickland,³⁶ B.Stoyanov,⁴¹ A.Straessner,¹⁸ K.Sudhakar,¹⁰ G.Sultanov,⁴¹ L.Z.Sun,²¹ S.Sushkov,⁸ H.Suter,⁴⁶ J.D.Swain,¹¹ Z.Szillasi,^{25,¶} X.W.Tang,⁷ P.Tarjan,¹⁶ L.Tauscher,⁵ L.Taylor,¹¹ B.Tellili,²³ D.Teyssier,²³ C.Timmermans,³⁰ Samuel C.C.Ting,¹⁴ S.M.Ting,¹⁴ S.C.Tonwar,^{10,18} J.Tóth,¹³ C.Tully,³⁶ K.L.Tung,⁷ J.Ulbricht,⁴⁶ E.Valente,³⁸ R.T.Van de Walle,³⁰ V.Veszpremi,²⁵ G.Vesztergombi,¹³ I.Vetlitsky,²⁷ D.Vicinanza,³⁹ G.Viertel,⁴⁶ S.Villa,³⁷ M.Vivargent,⁴ S.Vlachos,⁵ I.Vodopianov,³³ H.Vogel,³⁴ H.Vogt,⁴⁵ I.Vorobiev,^{34,27} A.A.Vorobyov,³³ M.Wadhwa,⁵ W.Wallraff,¹ X.L.Wang,²¹ Z.M.Wang,²¹ M.Weber,¹ P.Wienemann,¹ H.Wilkens,³⁰ S.Wynhoff,³⁶ L.Xia,³¹ Z.Z.Xu,²¹ J.Yamamoto,³ B.Z.Yang,²¹ C.G.Yang,⁵ H.J.Yang,³ M.Yang,⁷ S.C.Yeh,⁴⁹ An.Zalite,³³ Yu.Zalite,³³ Z.P.Zhang,²¹ J.Zhao,²¹ G.Y.Zhu,⁷ R.Y.Zhu,³¹ H.L.Zhuang,⁷ A.Zichichi,^{9,18,19} G.Zilizi,^{25,¶} B.Zimmermann,⁴⁶ M.Zöller,¹

- 1 I. Physikalisches Institut, RWTH, D-52056 Aachen, FRG[§]
III. Physikalisches Institut, RWTH, D-52056 Aachen, FRG[§]
- 2 National Institute for High Energy Physics, NIKHEF, and University of Amsterdam, NL-1009 DB Amsterdam, The Netherlands
- 3 University of Michigan, Ann Arbor, MI 48109, USA
- 4 Laboratoire d'Annecy-le-Vieux de Physique des Particules, LAPP,IN2P3-CNRS, BP 110, F-74941 Annecy-le-Vieux CEDEX, France
- 5 Institute of Physics, University of Basel, CH-4056 Basel, Switzerland
- 6 Louisiana State University, Baton Rouge, LA 70803, USA
- 7 Institute of High Energy Physics, IHEP, 100039 Beijing, China[△]
- 8 Humboldt University, D-10099 Berlin, FRG[§]
- 9 University of Bologna and INFN-Sezione di Bologna, I-40126 Bologna, Italy
- 10 Tata Institute of Fundamental Research, Mumbai (Bombay) 400 005, India
- 11 Northeastern University, Boston, MA 02115, USA
- 12 Institute of Atomic Physics and University of Bucharest, R-76900 Bucharest, Romania
- 13 Central Research Institute for Physics of the Hungarian Academy of Sciences, H-1525 Budapest 114, Hungary[†]
- 14 Massachusetts Institute of Technology, Cambridge, MA 02139, USA
- 15 Panjab University, Chandigarh 160 014, India.
- 16 KLTE-ATOMKI, H-4010 Debrecen, Hungary[¶]
- 17 INFN Sezione di Firenze and University of Florence, I-50125 Florence, Italy
- 18 European Laboratory for Particle Physics, CERN, CH-1211 Geneva 23, Switzerland
- 19 World Laboratory, FBLJA Project, CH-1211 Geneva 23, Switzerland
- 20 University of Geneva, CH-1211 Geneva 4, Switzerland
- 21 Chinese University of Science and Technology, USTC, Hefei, Anhui 230 029, China[△]
- 22 University of Lausanne, CH-1015 Lausanne, Switzerland
- 23 Institut de Physique Nucléaire de Lyon, IN2P3-CNRS, Université Claude Bernard, F-69622 Villeurbanne, France
- 24 Centro de Investigaciones Energéticas, Medioambientales y Tecnológicas, CIEMAT, E-28040 Madrid, Spain[♭]
- 25 Florida Institute of Technology, Melbourne, FL 32901, USA
- 26 INFN-Sezione di Milano, I-20133 Milan, Italy
- 27 Institute of Theoretical and Experimental Physics, ITEP, Moscow, Russia
- 28 INFN-Sezione di Napoli and University of Naples, I-80125 Naples, Italy
- 29 Department of Physics, University of Cyprus, Nicosia, Cyprus
- 30 University of Nijmegen and NIKHEF, NL-6525 ED Nijmegen, The Netherlands
- 31 California Institute of Technology, Pasadena, CA 91125, USA
- 32 INFN-Sezione di Perugia and Università Degli Studi di Perugia, I-06100 Perugia, Italy
- 33 Nuclear Physics Institute, St. Petersburg, Russia
- 34 Carnegie Mellon University, Pittsburgh, PA 15213, USA
- 35 INFN-Sezione di Napoli and University of Potenza, I-85100 Potenza, Italy
- 36 Princeton University, Princeton, NJ 08544, USA
- 37 University of California, Riverside, CA 92521, USA
- 38 INFN-Sezione di Roma and University of Rome, “La Sapienza”, I-00185 Rome, Italy
- 39 University and INFN, Salerno, I-84100 Salerno, Italy
- 40 University of California, San Diego, CA 92093, USA
- 41 Bulgarian Academy of Sciences, Central Lab. of Mechatronics and Instrumentation, BU-1113 Sofia, Bulgaria
- 42 The Center for High Energy Physics, Kyungpook National University, 702-701 Taegu, Republic of Korea
- 43 Purdue University, West Lafayette, IN 47907, USA
- 44 Paul Scherrer Institut, PSI, CH-5232 Villigen, Switzerland
- 45 DESY, D-15738 Zeuthen, FRG
- 46 Eidgenössische Technische Hochschule, ETH Zürich, CH-8093 Zürich, Switzerland
- 47 University of Hamburg, D-22761 Hamburg, FRG
- 48 National Central University, Chung-Li, Taiwan, China
- 49 Department of Physics, National Tsing Hua University, Taiwan, China

[§] Supported by the German Bundesministerium für Bildung, Wissenschaft, Forschung und Technologie
[†] Supported by the Hungarian OTKA fund under contract numbers T019181, F023259 and T024011.
[¶] Also supported by the Hungarian OTKA fund under contract number T026178.
[♭] Supported also by the Comisión Interministerial de Ciencia y Tecnología.
[#] Also supported by CONICET and Universidad Nacional de La Plata, CC 67, 1900 La Plata, Argentina.
[△] Supported by the National Natural Science Foundation of China.

\sqrt{s} (GeV)	191.6	195.5	199.5	201.7	203.8	205.1	206.3	206.6	208.0	208.6
Luminosity (pb $^{-1}$)	29.4	83.7	82.8	37.0	7.6	68.1	66.9	63.7	8.2	0.1

Table 1: The average centre-of-mass energies and corresponding integrated luminosities.

	N_D	N_B	$q\bar{q}(\gamma)$	WW	$Z e^+ e^-$	ZZ
Preselection	17719	17739.2	11364.2	5876.7	139.4	358.9
Selection	28	31.0	30.5	0.2	0.1	0.2

Table 2: Number of events, N_D , observed in data by the $q\bar{q}\gamma\gamma$ selection, compared with the Standard Model expectations, N_B . The Monte Carlo breakdown in different processes is given.

	N_D	N_B	$e^+e^-(\gamma)$	$\mu^+\mu^-(\gamma)$	$\tau^+\tau^-(\gamma)$	4 fermion
Preselection	738	751.3	541.7	46.2	50.4	113.0
Selection	7	8.0	4.2	1.8	2.0	0.0

Table 3: Number of events, N_D , observed in data by the $\ell^+\ell^-\gamma\gamma$ selection, compared with the Standard Model expectations, N_B . The Monte Carlo breakdown in different processes is given.

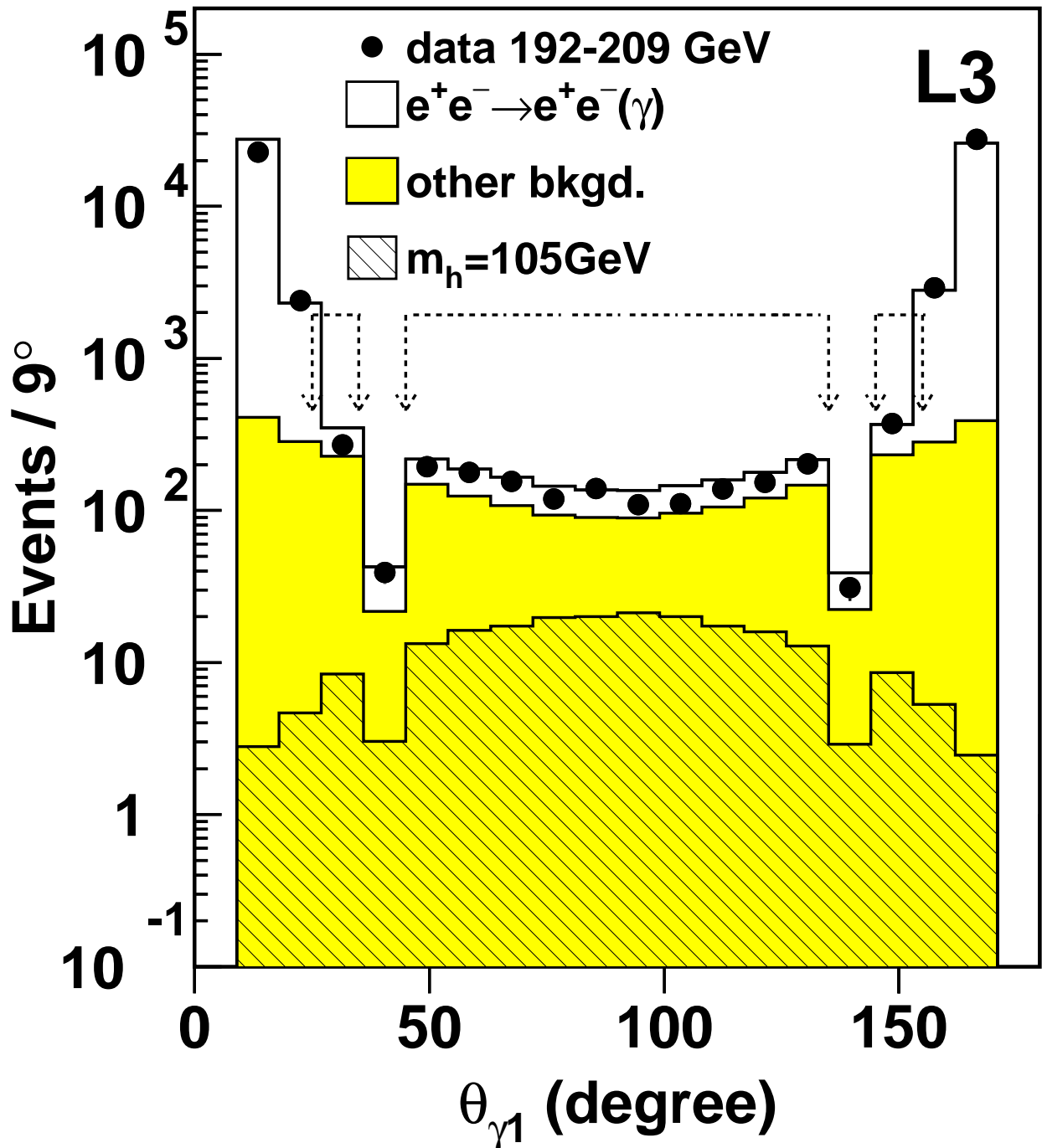


Figure 1: Distribution of the polar angle, $\theta_{\gamma 1}$ of the most energetic photon for data and background. A Higgs boson signal with mass $m_h = 105\text{ GeV}$ is superimposed with arbitrary normalisation. All Z final states are combined. The selected regions are indicated by the arrows.

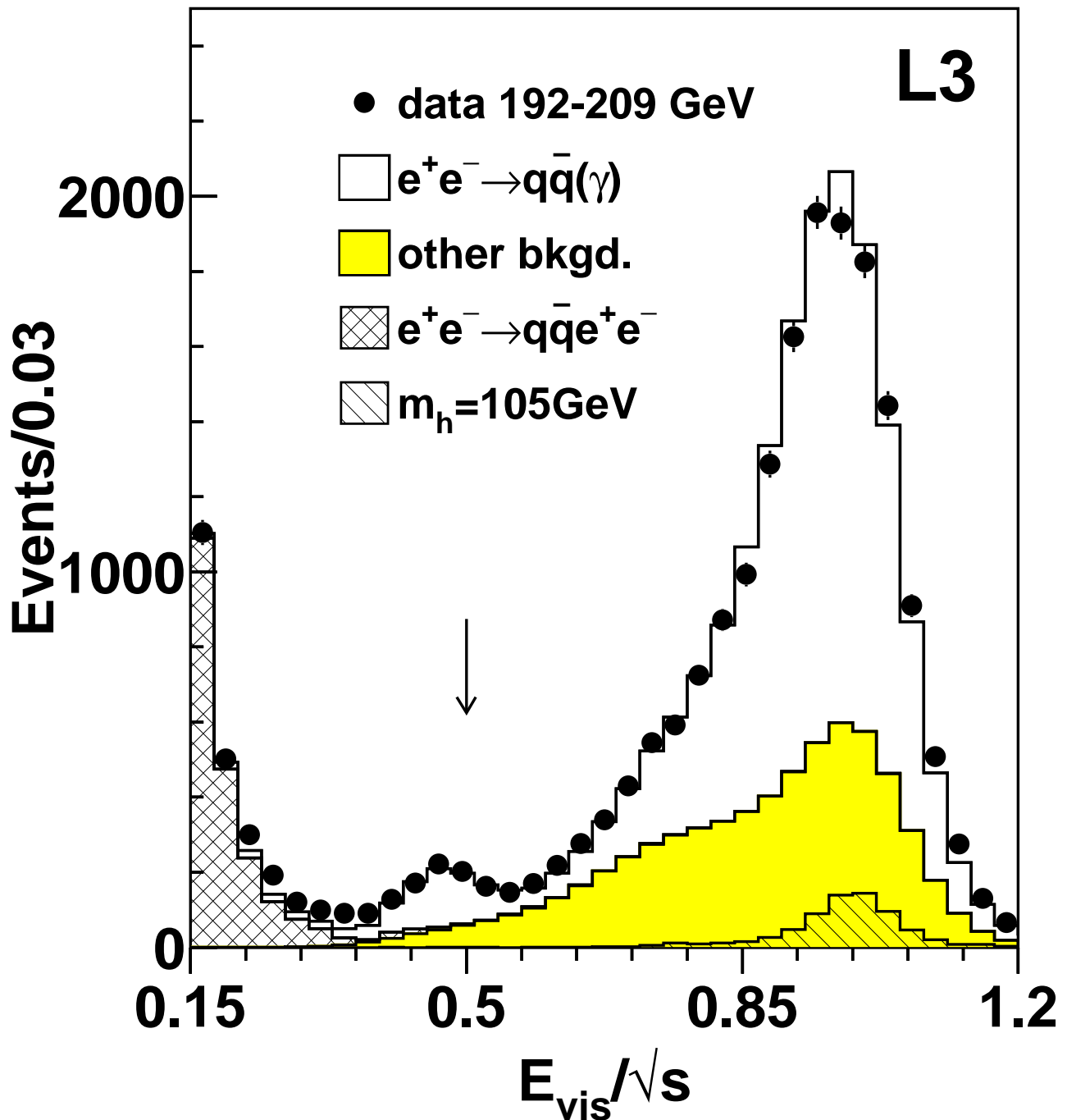


Figure 2: Distribution of E_{vis}/\sqrt{s} after the hadronic preselection for data and background for the $q\bar{q}\gamma\gamma$ final state. A Higgs boson signal with mass $m_h = 105$ GeV is superimposed with arbitrary normalisation. The arrow indicates the value of the cut.

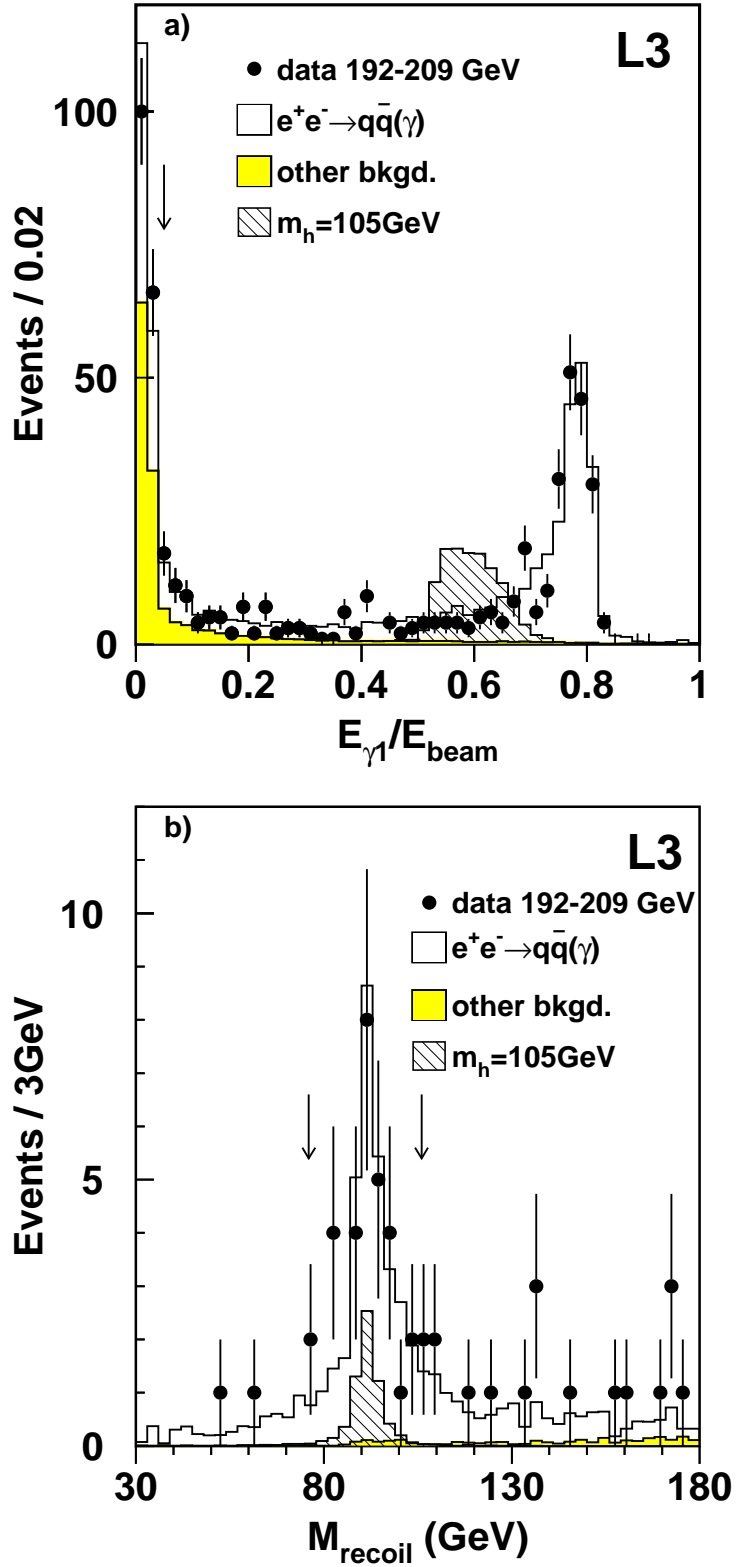


Figure 3: Distributions for the $q\bar{q}\gamma\gamma$ final state of a) the energy of the most energetic photon normalised to the beam energy and b) the recoil mass against the di-photon system in data, background and for a 105 GeV Higgs boson signal with arbitrary normalisation. The arrows indicate the values of the applied cuts.

Run # 852001 Event # 2399

$$M_{\gamma\gamma} = 111.8 \pm 1.0 \text{ GeV}$$
$$M_{\text{jetjet}} = 87.1 \pm 0.8 \text{ GeV}$$

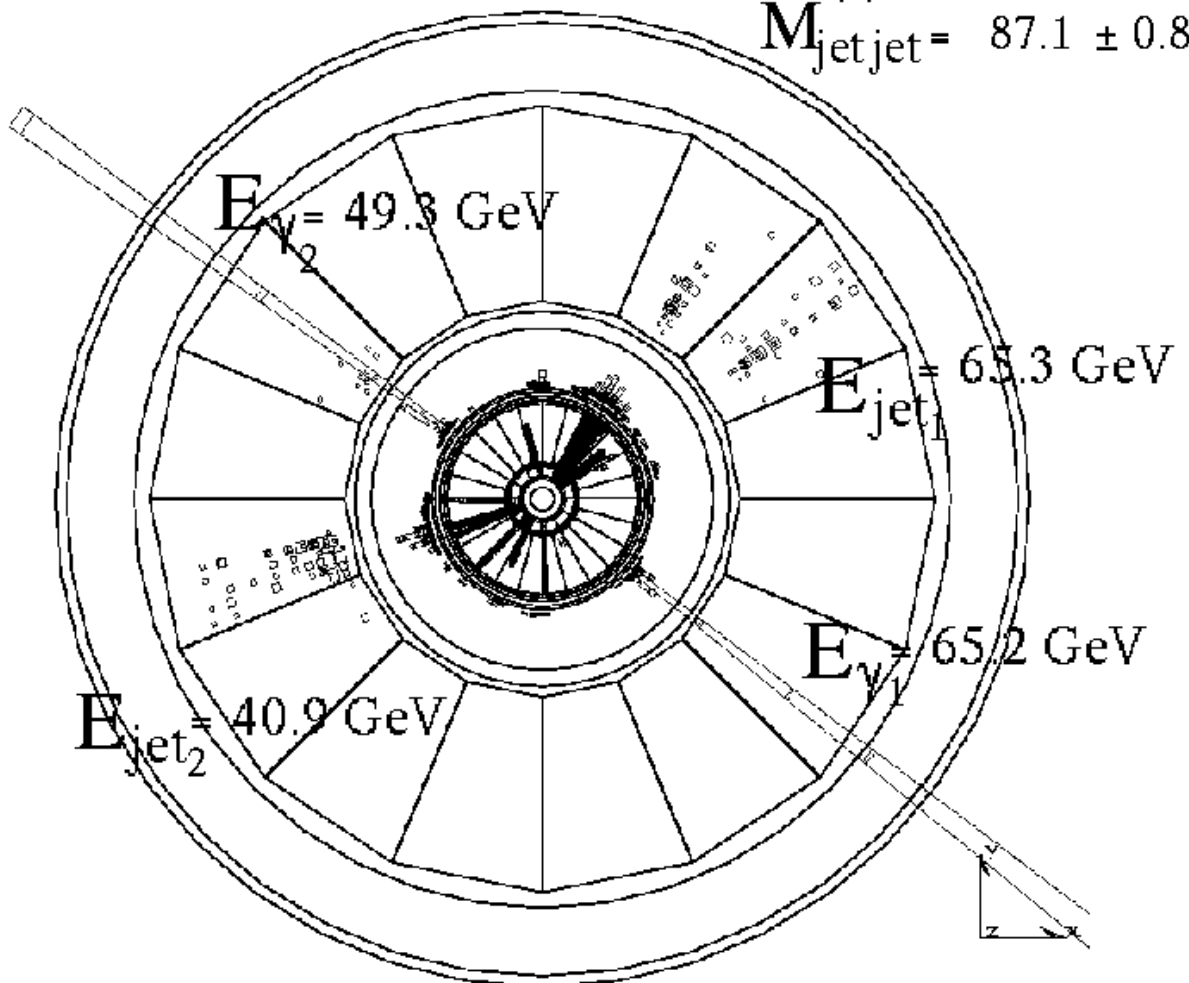


Figure 4: The $e^+e^- \rightarrow Z h \rightarrow q\bar{q}\gamma\gamma$ candidate with the highest di-photon invariant mass.

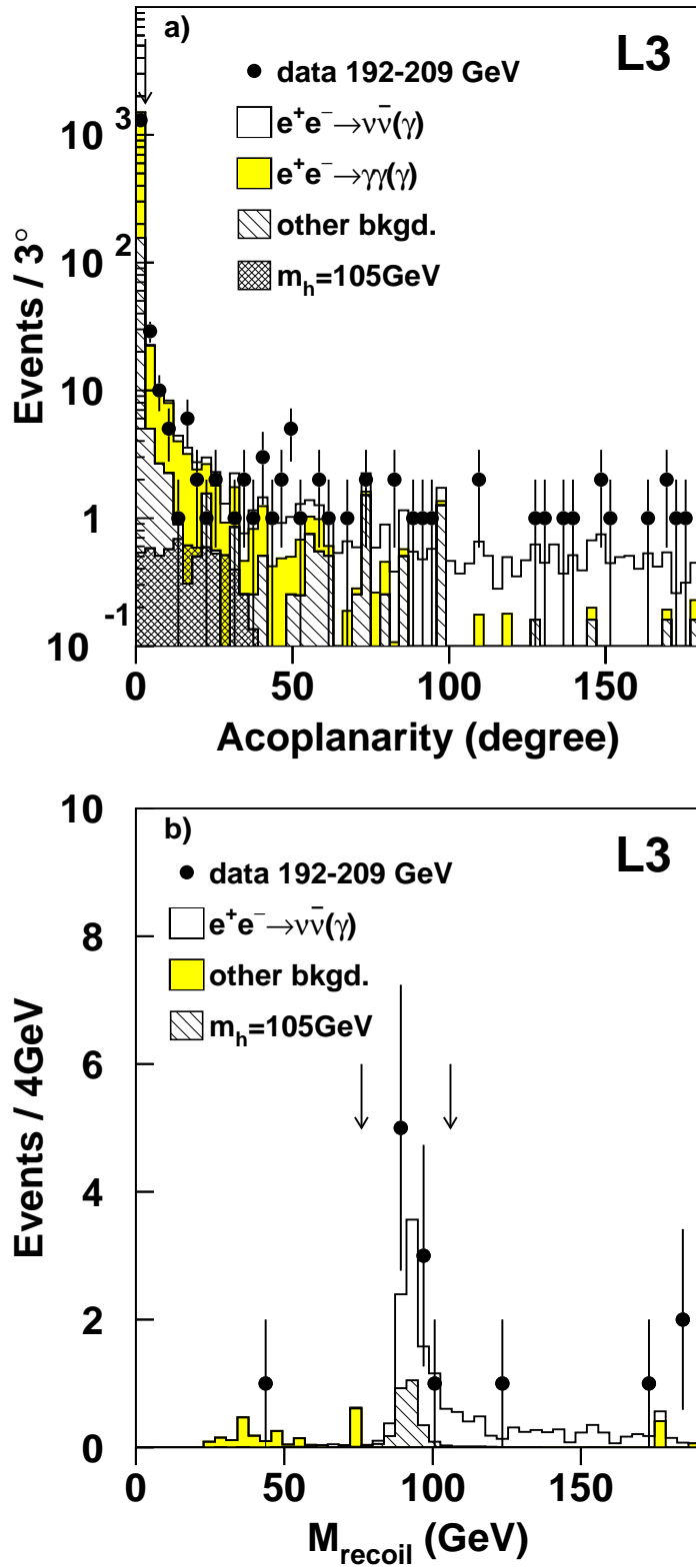


Figure 5: Distributions for the $\nu\bar{\nu}\gamma\gamma$ final state of a) the acoplanarity of the $\gamma\gamma$ system and b) the recoil mass against the two photons in data, background and for a Higgs boson signal with mass $m_h = 105$ GeV with arbitrary normalisation. The arrows indicate the values of the cuts.

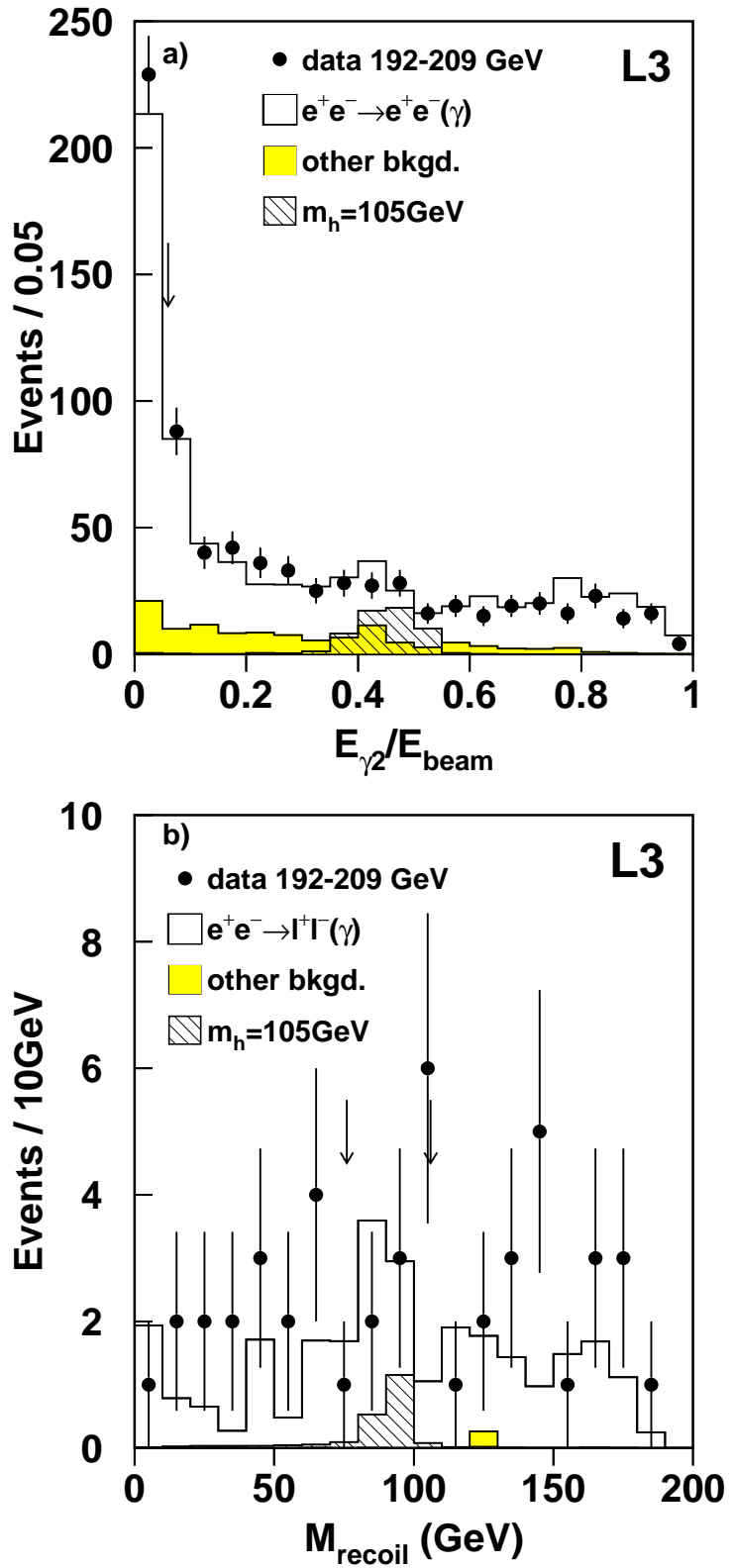


Figure 6: Distributions for the $\ell^+\ell^-\gamma\gamma$ final state of a) the energy of the second most energetic photon normalised to the beam energy, for the preselected events, and b) the recoil mass against the two photons. Data, background and a Higgs boson signal with mass $m_h = 105$ GeV and arbitrary normalisation are shown. The arrows indicate the values of the cuts.

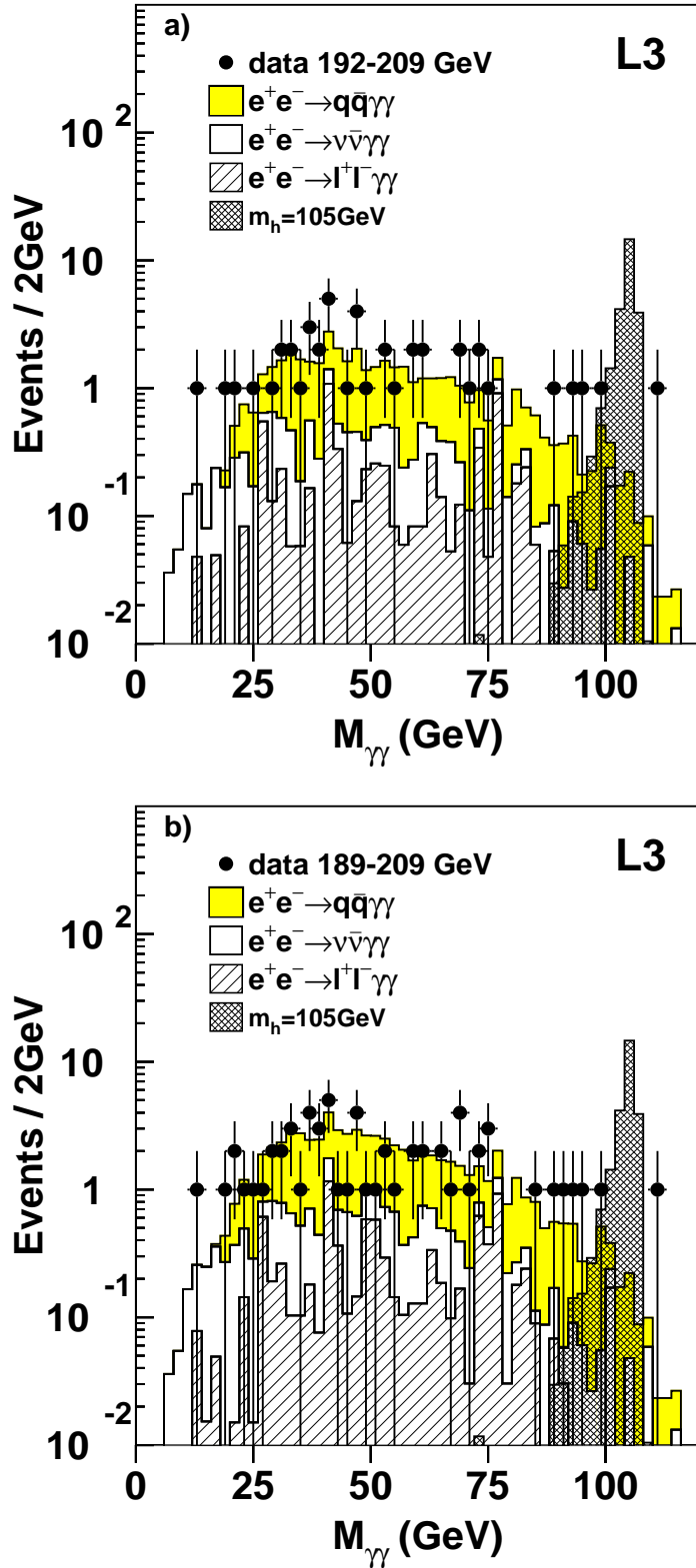


Figure 7: Distributions of the reconstructed di-photon invariant mass for all final states combined, after the final selection. Data at a) $\sqrt{s} = 192 - 209$ GeV, and b) $\sqrt{s} = 189 - 209$ GeV are shown together with the background and a Higgs boson signal with mass $m_h = 105$ GeV. The Standard Model cross section and a $\text{BR}(h \rightarrow \gamma\gamma) = 1$ are used.

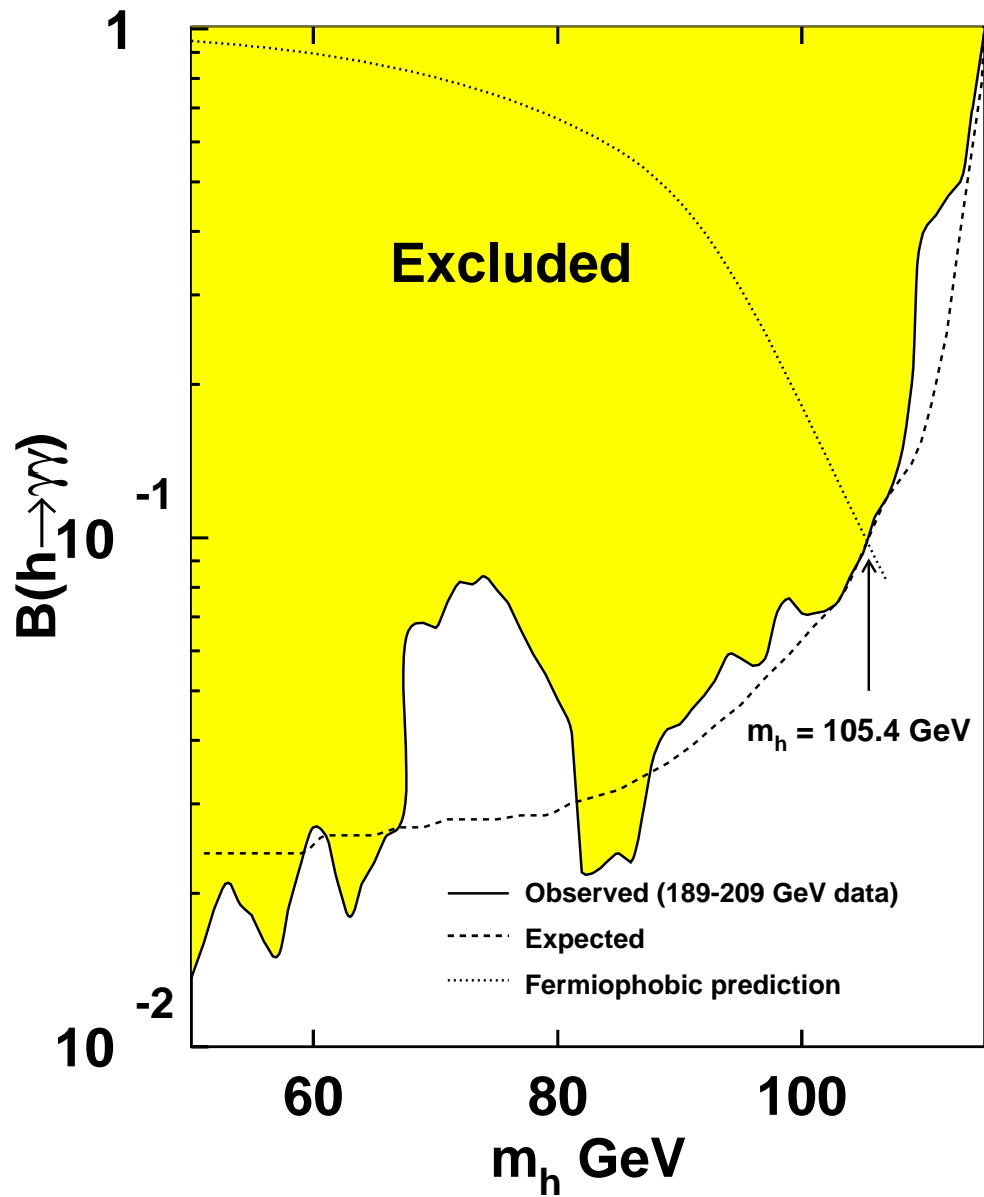


Figure 8: Excluded values at 95% confidence level of $\text{BR}(h \rightarrow \gamma\gamma)$ as a function of the Higgs mass, in the assumption of the Standard Model production cross section. The expected 95% confidence level limit and the theoretical prediction are also presented.